ELSEVIER

www.elsevier.nl/locate/jorganchem

Journal of Organometallic Chemistry 612 (2000) 1–8

Journal of Organo metallic Chemistry

^{57}Fe-Mössbauer spectroscopic study of monomeric and polymeric ferrocenyl- and octamethylferrocenyl-substituted ethynes

Herwig Schottenberger [a], Michael R. Buchmeiser [b], Rolfe H. Herber [c,*]

[a] *Institute of General, Inorganic and Theoretical Chemistry, University of Innsbruck, Innrain 52 a, A-6020 Innsbruck, Austria*
[b] *Institute of Analytical Chemistry and Radiochemistry, University of Innsbruck, Innrain 52 a, A-6020 Innsbruck, Austria*
[c] *Racah Institute of Physics, Hebrew University, 91904 Jerusalem, Israel*

Received 11 January 2000; accepted 19 April 2000

Abstract

A series of four monomeric and four polymeric ferrocenyl- and octamethylferrocenyl-substituted 1-alkynes, ethynylferrocene (**1**) [1271-47-2], 2-ethynylphenylferrocene (**2**) [1292-14-4], [2-[ethynylphen-2-yl]ethen-1-yl]-1′,2,2′,3,3′,4,4′,5-octamethylferrocene (**3**), novel [2-[ethynylphen-2-yl]ethen-1-yl]-1′,2,2′,3,3′,4,4′,5-octamethylferricinium hexafluorophosphate (**4**) and poly(ethynylferrocene) (**5**) [33410-56-9], poly(2-ethynylphenylferrocene) (**6**) [205865-61-8], poly([2-[ethynylphen-2-yl]ethen-1-yl]-1′,2,2′,3,3′,4,4′,5-octamethylferrocene) (**7**), and novel poly([2-[ethynylphen-2-yl]ethen-1-yl]-1′,2,2′,3,3′,4,4′,5-octamethylferricinium hexafluorophosphate) (**8**), have been studied by temperature-dependent ^{57}Fe-Mössbauer spectroscopy. The relevant Mössbauer parameters have been determined and are compared with the data obtained for the model compound octamethylferrocene (OMF). The data obtained by ^{57}Fe-Mössbauer spectroscopy reflect a small decrease of s-electron density from the ferrocene moiety to the conjugated backbone, as is demonstrated by the smaller IS of the monomers **1**–**3** in comparison with the corresponding polymers **5**–**7**. As may be deduced from the temperature dependence of the recoil-free fraction and the calculated lattice temperatures, the polymers are much 'softer' (within the definitions of Mössbauer spectroscopy) than the corresponding monomers. Finally, an unusual phase transition has been observed in OMF some 80°C below the melting point, which appears to lead to a large, sudden, and unexpected increase in the mean-square-amplitude of vibration of the metal atom in methyl substituted ring systems. This anomalous T-dependence of the recoil-free fraction, which is associated with the presence of the ring methyl groups, is not observed when one (or more) of the ring protons is replaced by a sterically bulky side chain, as in **1**–**3**. © 2000 Elsevier Science B.V. All rights reserved.

Keywords: Ferrocenyl polymers; Octamethyl ferrocenyl polymers; T-dependent; Mössbauer spectroscopy; Ethynes

1. Introduction

Polymeric metallocenes, including their cationic forms [1], have attracted significant interest during the last few years. In general, fully conjugated polymers based on poly-ynes [2], poly-enynes [3] or poly-enes [4] represent interesting materials for many applications in the fields of organic conductivity [5–9], optoelectronics and photonics [10–16]. Besides the use of substituted cycloactatetraenes [17–20], another attractive access to conjugated polyenes lies in the use of terminal acetylenes. These compounds are polymerized preferably by polymerizations using well-defined Schrock-type metathesis catalysts [21–31]. In general, the actual number of conjugated double bonds (usually expressed as N_{eff}) in these materials strongly depends on the electronic, as well as steric, nature of the substituents in the starting alkyne. Additionally, 1,3-interactions were found to play an important role [30]. Conjugated organometallic materials (such as polyenes), which contain pendant metallocenes, are believed to have great potential for high second- and third-order nonlinearities for three main reasons: (i) metallocenes show M–L (metal-to-ligand) and L–M (ligand-to-metal) charge transfer absorptions in the UV–vis region, transitions that are often associated with large second order nonlinearities; (ii) metallocenes often have high transition dipole moments, which lead to high second-order non-

---

* Corresponding author. Tel.: +972-2-6584244; fax: +972-2-6586347.

E-mail address: herber@vms.huji.a.il (R.H. Herber).

PII: S0022-328X(00)00280-1

linearities, and (iii) metallocenes are often stable in oxidation states that differ by one electron, and therefore can give rise to charged polymers. Due to the fact that ferrocene- and especially octa- and nonamethylferrocene derivatives are known to possess a pronounced Lewis base character, a significant charge transfer from the metallocene moiety to the conjugated backbone may be expected. In the case where such an electron transfer takes place, and where the corresponding polyene possesses sufficient coplanarity, bathochromic shifts in absorption associated with large values for the extinction coefficient (ε) may be observed [29,30]. Nevertheless, besides cyclic voltammetry (CV) there exist few analytical tools which are capable of providing quantitative information concerning the electron donating part of the metallocene or which at least allow an estimate of the actual electronic influence of such a pendant metallocene unit onto a conjugated polymer.

Recently, ^{57}Fe-Mössbauer spectroscopy has been used to elucidate the significance and extent of direct interactions between the iron atom and the corresponding bridge in ring-tilted [2]ferrocenophane systems [32] as well as in the investigation of ferrocenyl-substituted allenes and cummulenes [33,34]. In this contribution, the effect of the iron atom on the transformation of the monomeric compound into a polymer has been investigated by means of ^{57}Fe-Mössbauer spectroscopy, particularly the differences between monosubstituted and nonasubstituted monomeric and polymeric ferrocenes, as well as the lattice-dynamical consequences of the polymerization. In addition, the Mössbauer data of related polycationic species have been acquired, and will be described in detail below.

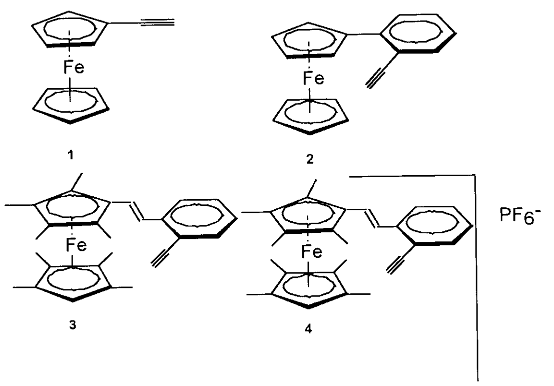

Fig. 1. Monomers **1**–**4**.

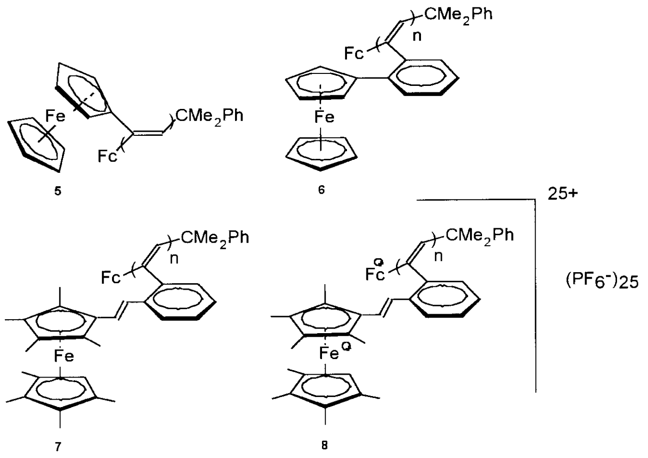

Fig. 2. Polymers **5**–**8**.

2. Experimental

2.1. Monomers and polymers

The ethynyl group containing monomers discussed in the present study are summarized graphically in Fig. 1, and the polymers in Fig. 2, and their preparation is discussed below. In addition, octamethyl ferrocene (OMF) [59568-28-4] was repeatedly recrystallized from hexane and showed a melting point of 431 K. Compounds **1** [1271-47-2], **2** [1292-14-4] and **3** as well as compounds **5** [33410-56-9], **6** [205865-61-8] and **7** were prepared as described previously [29,30,35,36]. Polymers **5**–**7** were prepared in benzene at room temperature (r.t.) from monomers **1**–**3** using $Mo(N\text{-}2,6\text{-}Me_2C_6H_3)(CHCMe_2Ph)(OCMe(CF_3)_2)_2$ as an initiator. End-capping of the living polymers was achieved using ferrocenecarbaldehyde. The general properties of these polymers have previously been reported [35] and a summary of the relevant polymer data is included in Table 2. The purity of monomers **1**, **2**, and **3** was checked by NMR and elemental analysis. Polymers **5**–**7** were fully characterized by GPC, NMR and FTIR.

2.2. [2-[Ethynylphen-2-yl]ethen-1-yl]-1′,2,2′,3,3′,4,4′,5-octamethylferricinium hexafluorophosphate (*4*)

Compound **3** (100 mg, 0.236 mmol) was suspended in acetonitrile (5 ml) and a solution of ferricinium hexafluorophosphate (120 mg, 0.230 mmol) in 2 ml of acetonitrile was added. The reaction mixture was stirred at r.t. for 1 h, diethyl ether (10 ml) was added and the precipitate was collected by means of filtration. Extensive washing with diethyl ether yielded **4** as a black solid. IR (KBr): 2295 w, 1150 m, 960 w, 850 b, vs (PF_6), 750 m. Anal. Calc. for $C_{28}H_{32}F_6FeP$ ($M_w = 569.150$): C, 59.04; H, 5.67; N, 0.00. Found: C, 58.6; H, 5.4; N, 0.0%.

2.3. Poly([2-[ethynylphen-2-yl]ethen-1-yl]-1′,2,2′,3,3′,4,4′,5-octamethylferri-cinium hexafluorophosphate) (*8*)

This compound was prepared starting from **7** according to the procedure described for the preparation of **4**,

Table 1
Mössbauer data for monomers **1**–**4**

Compound	Ferrocene	Octamethyl-ferrocene	Ethynyl-ferrocene (**1**)	2-Ethynylphenyl-ferrocene (**2**)	[2-[Ethynylphen-2-yl]-ethen-1-yl]-octamethylferrocene (**3**)	[2-[Ethynylphen-2-yl]-ethen-1-yl]-octamethylferricinium PF_6^- (**4**)
IS (90) (mm s^{-1})	0.531 ± 0.001	0.520 ± 0.003	0.524 ± 0.003	0.516 ± 0.001	0.507 ± 0.003	0.62 ± 0.02
QS (90) (mm s^{-1})	0.2491 ± 0.001	2.577 ± 0.00	2.343 ± 0.001	2.352 ± 0.002	2.395 ± 0.002	
dIS/dT (mm s^{-1} $K \times 10^4$)	3.292 ± 0.074	4.241 ± 0.080	3.86 ± 0.09		Non-linear	
dQS/dT (mm s^{-1} $K \times 10^4$)	1.861 ± 0.276	2.93 ± 0.13				
$-d \ln (A)/dT$ ($K^{-1} \times 10^3$)	8.50 ± 0.42	5.05 ± 0.37			7.97 ± 0.22	7.93 ± 0.52
M_{eff} (Da)	126	98.1	108	105		
Θ_M (K)	85	125	102	99		
M.p. (K)		431	325	344–349		

Table 2
Mössbauer data for polymers **5**–**8** [a]

Compound	Poly(ethynyl-ferrocene)$_{70}$ (**5**)	Poly(2-ethynylphenyl-ferrocene)$_{55}$ (**6**)	Poly([2-[ethynylphen-2-yl]ethen-1-yl]-octamethylferrocene)$_{25}$ (**7**)	Poly([2-[ethynylphen-2-yl]ethen-1-yl]-octamethylferricinium $PF_6^-)_{25}^+$ (**8**)
Polymer data	$M_w = 15\,000$ (D) PDI = 1.50 $\lambda_{max} = 440$ (shoulder) [b] (nm)	$M_w = 19\,200$ (D) PDI = 1.22 $\lambda_{max} = 511$ [b] (nm)	$M_w = 9800$ (D) PDI = 1.90 $\lambda_{max} = 500$ [b] (nm)	$M_w = 14\,555$ (Calc.) (D) PDI = n.d. $\lambda_{max} = 330, 390$ (shoulder) [c] (nm)
IS (90) (mm s^{-1})	0.535 ± 0.002	0.531 ± 0.001	0.513 ± 0.001	0.576 ± 0.010
QS (90) (mm s^{-1})	2.396 ± 0.002	2.405 ± 0.001	2.396 ± 0.004	
dIS/dT (mm s^{-1} $K \times 10^4$)	3.597 ± 0.133	3.82 ± 0.07	3.33 ± 0.18	
dQS/dT (mm s^{-1} $K \times 10^4$)	1.936 ± 0.159	1.56 ± 0.15	Non-linear	
$-d \ln (A)/dT$ ($K^{-1} \times 10^3$)	9.709 ± 0.287	11.01 ± 0.21	14.2 ± 0.7	
M_{eff} (Da)	116	109	~137	
Θ_M (K)	83.2	80.4	~63	
M.p. (K)				

[a] Fc = ferrocene.
[b] In THF.
[c] In methylene chloride.

using a solvent mixture of methylene chloride and acetonitrile (1:1) as a solvent. IR (KBr): 2295 w, 1152 m, 966 w, 845 b, vs (PF_6), 754 m.

2.4. ^{57}Fe Mössbauer spectroscopy

^{57}Fe Mössbauer spectroscopy was carried out using a source of ^{57}Co in a rhodium matrix (Isoflex, Moscow), as described previously [34]. All IS are reported with respect to the centroid of a r.t. spectrum of an 18 mg cm^{-2} metallic iron absorber, which was also used for spectrometer calibration. For T in the range 90–200 K, an excess of 10^6 counts per chanel (of 256) were recorded in each spectrum. At higher temperatures, where the f-factor becomes very small, up to 8×10^6 counts were recorded to reduce the statistical errors inherent in the data. Experimental errors of the reported parameters were calculated using standard propagation of error techniques and reflect a $\pm 1\sigma$ confidence level. In order to maximize random crystallite orientations with respect to the optical axis of the γ ray experiment, the microcrystalline powders were thoroughly mixed with roughly equal weight amounts of BN prior to packing in sample holders.

3. Results and discussion

The ^{57}Fe Mössbauer spectra of all of the compounds involved in the present study — except for the cationic complexes **4** and **8** — consist of well resolved doublets at all temperatures over the range 90–300 K, and a typical spectrum is shown in Fig. 3. The most important parameters, which may be extracted from ^{57}Fe Mössbauer spectroscopy are the isomeric shift (IS), the quadrupole splitting (QS) and the corresponding temperature-dependent values, dIS/dT, dQS/dT, as well as $-d \ln A/dT$. Moreover, using these parameters it is possible to extract [37] an 'effective vibrating mass', M_{eff}, and a 'Mössbauer lattice temperature', Θ_M, which help to characterize the compound in question. The isomer shift can be correlated with the s-electron density at the metal atom nucleus; an increase in the IS implies a decrease in the electron density, and vice versa. Consequently, any Lewis-base-related change in the electron density from the ferrocenyl moiety to the conjugated backbone should be reflected in the IS. The detailed results of the Mössbauer measurements for both the monomers and polymers will be briefly considered below, and the pertinent parameters are summarized in Table 1. The Mössbauer data for ferrocene, included in Table 1 for comparison, have been reported in detail in an earlier publication [32].

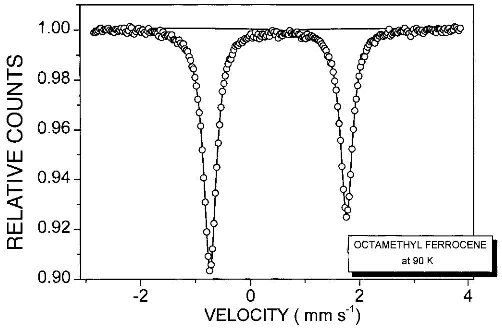

Fig. 3. Mössbauer spectrum of octamethyl ferrocene (OMF) at 90 K. The intensity asymmetry is temperature independent and arises from preferential crystallite orientation with respect to the optical axis.

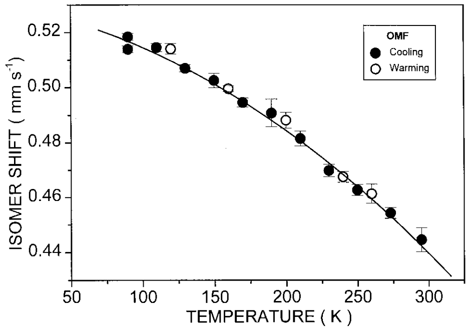

Fig. 4. Temperature dependence of the isomer shift for OMF. The error bars are those of the individual data points. The solid line represents the second-order polynomial regression through the data points.

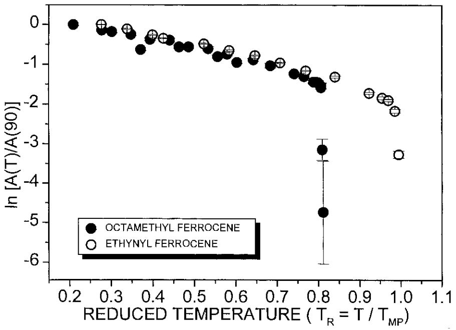

Fig. 5. The temperature dependence of the recoil-free fraction for OMF and **1**.The abscissa is the reduced temperature, $T_R = T/T_{MP}$, where the melting points are those of OMF and **1**, respectively. The large error bars of the highest temperature measurements reflect the very small values of the resonance effect magnitude, although in excess of 8×10^6 counts per channel were acquired in the individual experiments.

3.1. Octamethyl ferrocene (OMF)

The ^{57}Fe-Mössbauer parameters of this compound have been investigated in considerable detail, since OMF can serve as a reference (model) compound with respect to the other monomers and polymers included in this study, as well as the fact that OMF displays a number of interesting properties in its own right.

A typical spectrum of **1** (at 90 K) is shown in Fig. 3, and the 90 K hyperfine parameters are included in Table 1. The temperature dependence of the IS is shown in Fig. 4, in which a small amount of curvature is evident. However, fitting these data to a linear regression ($-\mathrm{d}IS/\mathrm{d}T = (4.241 \pm 0.080) \times 10^{-4}$ mm s^{-1} K^{-1} with a correlation coefficient of 0.996 for 26 data points) leads to a value of $M_{\mathrm{eff}} = 98$ Da, in reasonable agreement with data for the ring-substituted ferrocenes reported earlier [37]. The temperature dependence of the QS hyperfine interaction can be fitted by a reasonably linear regression ($-\mathrm{d}QS/\mathrm{d}T = (2.93 \pm 0.13) \times 10^{-4}$ mm s^{-1} K^{-1}, cc:0.98 for 25 data points) over the entire temperature range. While these data are unexceptional for ring-substituted ferrocenes, the temperature dependence of the recoil-free fraction (as reflected in the area under the resonance curve for a thin absorber) is markedly anomalous, as indicated in Fig. 5, in which the abscissa is expressed in terms of the reduced temperature $T_R = T/T_{MP}$. From this figure it is seen that while $\ln A(T)$ is reasonably linear in the range $90 \leq T \leq 347$ K, the resonance effect abruptly disappears above 350 K (T_R 0.82), that is, some 80°C below T_{mp}. This is in marked contrast to the related octamethyl ferrocenyl complexes as will be discussed. The onset of the reduction of the resonance effect is unusually sharp, and appears to involve a hysteresis, since it is necessary to cool the sample (from slightly above 350 K to about 330 K) before the resonance effect can again be observed. These observations suggest the presence of a first-order transition, but it should be noted that this is probably not a simple crystallographic phase transition, since there is no shattering of the crystallites when these are warmed through the 350 K point. The drastic decrease in the resonance effect on warming must be associated with the onset of a motion (or motions) of the Cp-rings, which permits a large increase in the mean-square-amplitude of vibration of the metal atom above 350 K. At this point it might be speculated that this Cp-ring motion is associated with the presence of two rings, neither of which has a ring substituent larger

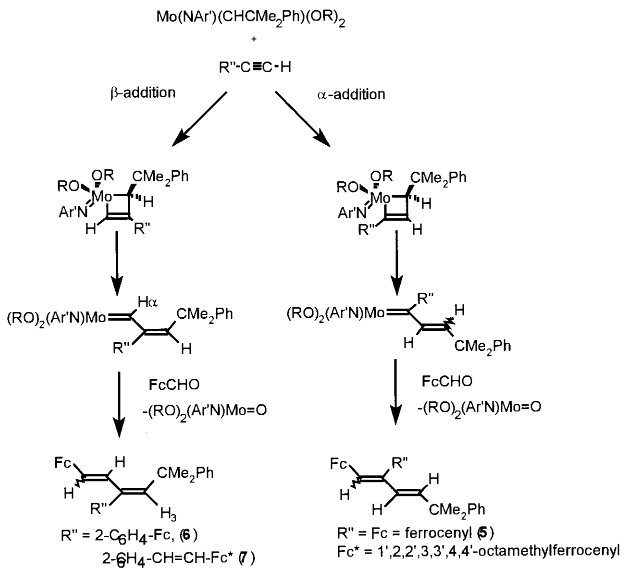

Scheme 1. Preparation of polymers **5**–**7**.

than a methyl group, but appears not to be observed in the absence of these ring substituent methyl groups. This point will be more fully addressed below.

The structures of monomers **1**–**4** as shown in Fig. 1 were chosen because they represent two sets of compounds. The first set consists of the simplest metallocenylalkyne, **1**, and a spacered homologue, **2**. The second represents the octamethyl-substituted analogues, **3** and **4**. In terms of polymer structures it is worth noting that poly-**1** (**5**) stems from an α insertion of **1** into the initiator, while poly-**2** and poly-**3** result from a β insertion [27,29,31,38]. A description of the polymerization and the resulting polymer structures is given in Scheme 1.

3.2. Compound *1*

The Mössbauer spectrum at 90 K of ethynyl ferrocene consists of a normal well-resolved doublet at all temperatures considered. The temperature dependence of the IS is similar to that shown in Fig. 4, and the slight curvature noted in these data suggest the participation of several vibrational modes in the motion of the central metal atom. Using a linear approximation to the data ($-\mathrm{dIS}/\mathrm{d}T = (3.86 \pm 0.09) \times 10^{-4}$ mm s^{-1} K^{-1} with a correlation coefficient of 0.996 for 15 data points) leads to a value of $M_{\mathrm{eff}} = 108$ Da. The difference between this value and the 'bare' iron atom mass of 57 Da reflects the covalent bonding of the metal atom to the Cp framework. The QS parameter for **1** is essentially temperature independent over the range $90 \leq T \leq 273$ K and has a mean value of 2.343 ± 0.001 mm s^{-1}.

The temperature dependence of the recoil-free fraction for **1** — as reflected in the area (A) under the resonance curve — is summarized graphically in Fig. 5 (in which the abscissa is the reduced temperature) and provides a comparison with the corresponding data for OMF. For **1**, the ln $A(T)$ data are nearly linear up to ~ 315 K ($T_{\mathrm{R}} \sim 0.97$), that is, to within less than 10 K of the melting point (324.5 K), reflecting the fact that no low frequency modes (libration or rotation) arising from ring motions play a dominant role in the metal atom motion, which is governed primarily by the Fe–Cp bonding interaction.

3.3. Compound *2*

The Mössbauer data for 2-ethynylphenylferrocene, for which a detailed crystal structure has been published [29], are very similar to those summarized for **1**, above. Although as usual there is some curvature in the IS(T) data, a linear regression ($-\mathrm{dIS}/\mathrm{d}T = (3.96 \pm 0.14) \times 10^{-4}$, with a correlation coefficient of 0.985 for 28 data points) leads to a value of $M_{\mathrm{eff}} = 105$ Da, and thus the addition of the phenyl group 'spacer' plays no significant role in the bonding of the metal atom to the Cp ligands. The temperature dependence of the recoil-free fraction is nearly linear ($90 \leq T \leq 340$ K) up to a reduced temperature of 0.99 ($T_{\mathrm{mp}} = 344$–346 K), and shows no anomalous behavior over this interval. Applying a linear regression to these data leads to a value of $\Theta_{\mathrm{M}} = 99$ K.

In the asymmetric unit of **2** there are two independent molecules, which differ greatly in their conformation — the two dihedral angles are 26.6(5) and 30.2(4)°. In the former conformation the triple bond points in the direction of the iron atom, in the latter, the molecule is twisted in the opposite direction. The distance between the acetylinic C atoms (C(17) and C(18) [29]) and the metal atom are 3.813(8) and 4.229(9) Å in one conformer, and 4.658(1) and 5.379(1) in the other. These distances are too long to permit a meaningful bonding interaction between the metal atom and the olefinic moiety and, not unexpectedly, the Mössbauer parameters are insensitive to the difference between the two conformers, and the data can be treated in terms of a single type of metal atom environment.

3.4. Compound *3*

The Mössbauer parameters for 1-octamethyl ferrocenyl 2 (2-ethynylphenyl)ethylene are summarized in Table 1. Again, although there is some curvature in the IS(T) data, a linear regression analysis ($-\mathrm{dIS}/\mathrm{d}T = (3.30 \pm 0.13) \times 10^{-4}$ mm s^{-1} K^{-1}, cc:0.990 for 15 data points) leads to an $M_{\mathrm{eff}} = 126$ Da. The QS hyperfine interaction is essentially T-independent, and has a mean value of 2.395 ± 0.003 mm s^{-1} over the range $90 < T < 328$ K. The temperature dependence of the

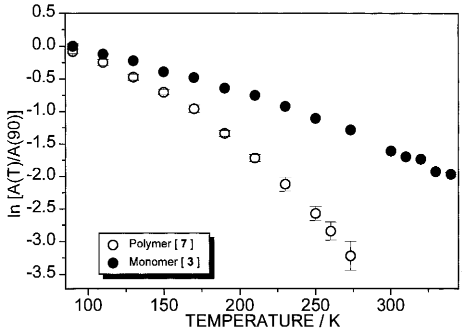

Fig. 6. The temperature dependence of the recoil-free fraction for compounds **3** and **7** showing the 'softer' lattice in the latter. The data have been normalized to the respective 90 K data points. The error bars reflect the errors in the individual data points.

recoil-free fraction for **3** is included graphically in Fig. 6 (vide infra, a comparison with the respective monomer/polymer data) from which it is noted that — although there is some 'softening' of the lattice starting at about 25°C below T_{mp} (330 K) — the resonance effect is readily observed to within 2°C of T_{mp}. This, of course, is in marked contrast to the data cited for OMF, above, in which the same two tetramethyl substituted ring moieties are present. In **3**, as is obvious, the presence of the large 2-ethynylphenylacetylene side chain apparently inhibits the onset of the ring motion, which has been identified with the large increase in the mean-square-amplitude of the metal atom motion above 350 K in OMF.

3.5. Compound 4

The 90 K Mössbauer spectrum of **4** is shown in Fig. 7. The spectral line shape is one which is characteristic of a relaxation spectrum with its broad non-Lorentzian appearance, and the data have been fitted with the relaxation program used earlier [37] (IS ~ 0.503(5) mm s^{-1} and QS ~ −0.19(1) mm s^{-1} at 90 K). The near collapse of the quadrupole interaction is due to the removal of one d-electron from the e_{2g} orbitals, which, in the case of the ferrocene–ferricinium absorbers, effectively removes 0.8064 of a $[3d_0>]$ electron, following the molecular orbital scheme of Dahl and Ballhausen [39,40]. However, this d-electron removal is expected to decrease the IS of the oxidized species relative to the neutral complex, whereas in the present case, the isomer shift increases by ~0.11 mm s^{-1} going from **3** to **4** both at 90 K. This increase in IS is in good agreement with the data for the ring-substituted ferrocene systems reported earlier [37].

The relaxation noted above is due to the interaction of the dilute unpaired electron spins with the lattice, similar to those which have been observed [37] for related ferricinium cationic absorbers and is presumed due to a Raman process (high *T* limit). Assuming a magnetic hyperfine field of 520 kOe (typical of Fe^{+3}), the calculated relaxation time at 90 K is 1.0×10^{-9} s. Finally, it is worth noting that the resonant effect in **4** is readily observable at temperatures well above 360 K, in contrast to the behavior of OMF detailed above, despite the presence of the eight methyl groups on the two Cp rings in both monomers. Moreover, the *T*-dependence of the recoil-free fraction for **3** and **4** are essentially identical; the one-electron oxidation, as well as the presence of the PF_6^- groups apparently has little effect on the metal atom dynamics in these two compounds. It is worth noting in this context that the corresponding data for $OMF^+PF_6^-$ similarly closely mimic those for neutral OMF. The coincidence of these two sets of data have a profound implication for the mechanism of the anomalous recoil-free fraction behavior, noted above for OMF, since it is clear that this phenomenon must be associated with an intra- rather

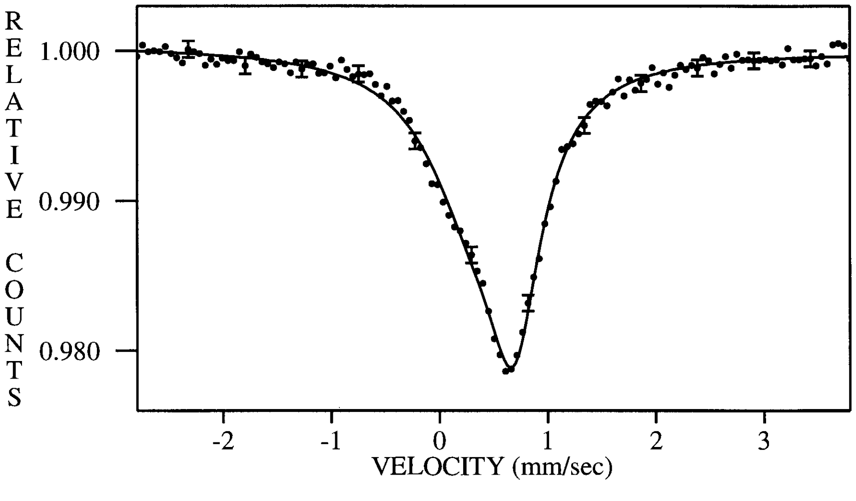

Fig. 7. Mössbauer Spectrum of **4** at 90 K typical of spin-lattice relaxation and a non-zero quadrupole hyperfine interaction in the solid. The magnetic hyperfine field assumed in the fitting procedure was 396 kOe.

than an intermolecular process, such as ring librational motion. The detailed structural implications of these observations are currently being studied in these laboratories.

3.6. Compound **5**

The Mössbauer parameters of **5** are included in Table 2 and are not otherwise exceptional. The IS(T), QS(T) and $\ln A(T)$ data are well fitted by linear regressions, and the M_{eff} and Θ_{M} data extracted from these dependencies are included in Table 2. It is interesting to note that these parameters are all very similar to those observed for the monomer **1** with the exception of the Mössbauer lattice temperature, which is some 20% lower in the polymer, indicating a 'softening' of the polymer lattice with respect to the monomer, presumably due to a larger density of states of low frequency vibrational motions in the latter with respect to the former. The small increase in the IS at 90 K in going from **1** to **5**, which is also noted for the other monomer–polymer pairs, suggests a small decrease in the s-electron density (at the metal atom site) in the polymer with respect to the monomer. The reasons for this change are not yet fully elucidated in the present instance.

3.7. Compound **6**

Comments similar to those articulated above for **5** apply to **6**, including the apparent 'softening' of the polymer lattice with respect to the monomer, and the appropriate parameters are included in Table 2.

3.8. Compound **7**

Again, the relevant hyperfine parameters for this polymer are included in Table 2. However, because of the significant curvature observed in both the IS(T) and $\ln a(T)$ data for this material, it is not possible to extract meaningful Θ_{M} and M_{eff} values in this case. However, a direct comparison of the recoil-free fraction data with those of the corresponding monomer **3** is shown in Fig. 6, from which the 'softening' of the polymer lattice relative to the monomer is clearly established by the larger slope in the former.

3.9. Compound **8**

The Mössbauer spectrum for this polymer is very similar to that of the corresponding monomer **4**, and consists of a single broadened line at an isomer shift of 0.576 at 90 K. Each of the iron atoms in the monomer has been oxidized to Fe^{+3}, and the quadrupole splitting has effectively collapsed, as noted above. The calculated relaxation rate at 90 K is 1.24×10^{-10} s.

4. Summary and conclusions

The hyperfine interactions and lattice dynamics of a number of ferrocenyl and octamethyl ferrocenyl substituted ethynes has been examined of the range $90 < T < 360$ K, and an unusual motional anomaly has been observed for OMF. The sudden increase in the mean-square amplitude of vibration of the metal atom can be associated with the presence of eight methyl substituents on the two Cp rings, but appears to be absent when the ninth ring position is occupied by a bulky organic group. Oxidation of the metal atom in monomer **3** leads to spin-lattice interactions in both the corresponding monomer cation complex, **4**, as well as in the corresponding polymer cation complex, **8**. The Mössbauer lattice temperature, Θ_{M}, as probed by the metal atom in these solids, decreases by 20–40% when the monomer is polymerized into an extended chain structure, presumably due to the influence of additional low-frequency vibrational modes on the metal atom motion. Polymerization of **1**–**3** to **5**–**7**, respectively, is reflected in a small decrease in the s-electron density at the metal atom nucleus, while the oxidation of **3** to **4** leads to a more significant decrease of this density, in agreement with earlier results on ring-substituted ferrocenes [37].

Acknowledgements

Financial support was provided by the Austrian National Science Foundation (FWF Vienna, project number P-12963-GEN) and the 'Jubiläumsfond der Österreichischen Nationalbank', Vienna, Austria, (project number 7489). This research has also been supported by a grant from the Israel Academy of Sciences, and is herewith gratefully acknowledged. The generous assistance of Professor I. Nowik in connection with evaluation of the relaxation spectra is also thankfully acknowledged.

References

[1] H. Schottenberger, M.R. Buchmeiser, Recent Res. Dev. Macromol. Res. 3 (1999) 535.
[2] T. Ogawa, Prog. Polym. Sci. 20 (1995) 943.
[3] S. Patai, Z. Rappoport, in: S. Patai (Ed.), The Chemistry of Triple-Bonded Functional Groups, Vol. Suppl. C2, Wiley, Chichester, UK, 1983, pp. 917–980.
[4] R. Lytel, G.F. Lipscomb, J. Thackara, J. Altman, P. Elizondo, M. Stiller, B. Sullivan, in: P.N. Prasad, D.R. Ulrich (Eds.), Nonlinear and Electro-Optic Organic Devices, Plenum, New York, 1987, p. 415.
[5] J. Zyss, D.S. Chemla, in: D.S. Chemla, J. Zyss (Eds.), Nonlinear Optical Properties of Organic Molecules and Crystals, vol. 1, Academic Press, Orlando, FL, 1987, p. 23.

[6] G. Yu, A. Heeger, The Physics of Semiconductors, vol. 1, World Scientific, Singapore, 1996.

[7] J. Vohlidal, J. Sedlácek, M. Pacovská, O. Lavastre, P.H. Dixneuf, H. Balcar, J. Pfleger, Polymer 38 (1997) 3359.

[8] P.N. Prasad, Polymer 32 (1991) 1746.

[9] T. Kobayashi, T. Hattori, A. Terasaki, K. Kurokawa, in: P.N. Prasad, D.R. Ulrich (Eds.), Femtosecond Studies of Dephasing and Phase Conjugation with Incoherent Light, Plenum, New York, 1987, p. 137.

[10] F. Meyers, S.R. Marder, B.M. Pierce, J.L. Brédas, J. Am. Chem. Soc. 116 (1994) 10703.

[11] J.L. Brédas, R. Silby, D.S. Boudreaux, R.R. Chance, J. Am. Chem. Soc. 105 (1983) 6555.

[12] T.J. Marks, M.A. Ratner, Angew. Chem. Int. Ed. Engl. 107 (1995) 167.

[13] C.B. Gormann, S.R. Marder, Chem. Mater. 7 (1995) 215.

[14] D.R. Kanis, M.A. Ratner, T.J. Marks, Chem. Rev. 94 (1994) 195.

[15] J.L. Brédas, Adv. Mater. 7 (1995) 262.

[16] F. Hide, M.A. Díaz-García, B.J. Schwartz, A. Heeger, J. Acc. Chem. Res. 30 (1997) 430.

[17] C.B. Gorman, E.J. Ginsburg, R.H. Grubbs, J. Am. Chem. Soc. 115 (1993) 1397.

[18] C.B. Gorman, E.J. Ginsburg, M.J. Sailor, J.S. Moore, T.H. Jozefiak, N.S. Lewis, R.H. Grubbs, S.R. Marder, J.W. Perry, Synth. Metals 41 (1991) 1033.

[19] M.J. Sailor, E.J Ginsburg, C.B. Gorman, A. Kumar, R.H. Grubbs, N.S. Lewis, Science 249 (1990) 1146.

[20] E.J. Ginsburg, C.B. Gorman, S.R. Marder, R.H. Grubbs, J. Am. Chem. Soc. 111 (1989) 7621.

[21] K. Knoll, S.A. Krouse, R.R. Schrock, J. Am. Chem. Soc. 110 (1988) 4424.

[22] S.A. Krouse, R.R. Schrock, Macromolecules 21 (1988) 1885.

[23] K.C. Wallace, A.H. Liu, W.M. Davis, R.R. Schrock, Organometallics 8 (1989) 644.

[24] R. Schlund, R.R. Schrock, W.E. Crowe, J. Am. Chem. Soc. 111 (1989) 8004.

[25] F.J. Schattenmann, R.R. Schrock, W.M. Davis, J. Am. Chem. Soc. 118 (1996) 3295.

[26] H.H. Fox, R.S. Schrock, Organometallics 11 (1992) 2763.

[27] R.R. Schrock, S. Luo, N. Zanetti, H.H. Fox, Organometallics 13 (1994) 3396.

[28] M. Buchmeiser, Macromolecules 30 (1997) 2274.

[29] M.R. Buchmeiser, N. Schuler, N. Kaltenhauser, K.-H. Ongania, I. Lagoja, K. Wurst, H. Schottenberger, Macromolecules 31 (1998) 3175.

[30] M. Buchmeiser, R.R. Schrock, Macromolecules 28 (1995) 6642.

[31] R.R. Schrock, S. Luo, J.C. Lee, Jr., N.C. Zanetti, W.M. Davis, J. Am. Chem. Soc. 118 (1996) 3883.

[32] R.H. Herber, K. Temple, I. Manners, M. Buretea, T.D. Tilley, Inorg. Chim. Acta 287 (1999) 152.

[33] V. Guillaume, P. Thominot, F. Coat, A. Mari, C. Lapinte, J. Organomet. Chem. 565 (1998) 75.

[34] R.H. Herber, B. Bildstein, P. Denifl, H. Schottenberger, Inorg. Chem. 36 (1997) 3586.

[35] M.R. Buchmeiser, N. Schuler, H. Schottenberger, I. Kohl, A. Hallbrucker, K. Wurst, Macromolecules (1999), in press.

[36] K. Wurst, O. Elsner, H. Schottenberger, Synlett (1995) 833.

[37] R.H. Herber, T.P. Hanusa, Hyperfine Interact. 108 (1997) 563.

[38] H.H. Fox, M.O. Wolf, R. O'Dell, B.L. Lin, R.R. Schrock, M.S. Wrighton, J. Am. Chem. Soc. 116 (1994) 2827.

[39] J.P. Dahl, C.F. Ballhausen, Mat. Fys. Medd. Dan. Vid. Selsk. 55 (1961) 5.

[40] N.N. Greenwood, T.C. Gibb, Mössbauer Spectroscopy, Chapman and Hall, London, 1971.